Quantum phase transitions of fermionic atoms in an anisotropic triangular optical lattice*

Bao An(保 安)[a)†], Chen Yao-Hua(陈耀桦)[b)], and Zhang Xiao-Zhong(章晓中)[a)]

[a)] *Laboratory of Advanced Materials, School of Materials Science and Engineering, Tsinghua University, Beijing* 100084, *China*

[b)] *Beijing National Laboratory for Condensed Matter Physics, Institute of Physics, Chinese Academy of Sciences, Beijing* 100190, *China*

(Received 4 March 2013; revised manuscript received 22 April 2013)

The effect of anisotropy caused by a confining potential on the properties of fermionic cold atoms in a triangular optical lattice is systematically investigated by using the dynamical cluster approximation combined with the continuous time quantum Monte–Carlo algorithm. The quantum phase diagrams which reflect the temperature–interaction relation and the competition between the anisotropic parameter and the interaction are presented with full consideration of the anisotropy of the system. Our results show that the system undergoes a transition from Fermi liquid to Mott insulator when the repulsive interaction reaches a critical value. The Kondo effect also can be observed in this system and the pseudogap is suppressed at low temperatures due to the Kondo effect. A feasible experiment protocol to observe these phenomena in an anisotropic triangular optical lattice with cold atoms is proposed, in which the hopping terms are closely related to the lattice confining potential and the atomic interaction can be adjusted via the Feshbach resonance.

Keywords: triangular optical lattice, cold atoms, cluster dynamical approximation

PACS: 03.75.Ss, 37.10.Jk, 32.80.Hd, 67.85.Lm **DOI:** 10.1088/1674-1056/22/11/110309

1. Introduction

Cold atoms in optical lattices with perfect structures and highly controllable parameters have been an ideal toolbox for the investigation of quantum many-body phenomena.[1–4] Many research studies based on cold atoms in optical lattices have been carried out and fruitful results have been obtained, such as the observation of the Mott insulator and superfluidity of strongly interacting fermions and the quantum phase transition between these novel states, the quantum simulations of the antiferromagnetic spin chains, the frustrated classical magnetism in a triangular optical lattice, Bose–Einstein condensation in optical lattices, and so forth.[5–12] It is known that the novel states, such as the spin liquid and the spin ice which are found in the frustrated systems, play a pivotal role in the understanding of the mechanisms of the high temperature superconductivity and magnetic monopoles. Therefore, many experimental and theoretical studies have focused on geometrically frustrated systems.[13–19] However, so far few works have been done on the anisotropic triangular lattice systems in which the anisotropy is related to the hopping terms in different directions.

Optical lattices with different structures and dimensions can be set up by overlapping several laser beams of the same frequency with different propagating directions.[20–26] The quantum simulating platform for an anisotropic triangular optical lattice can be achieved by interfering three coplanar (such as the xy plane) laser beams with the same frequency and different intensities, each separated by $2\pi/3$ and all of them being polarized in the z direction. The periodic confining potential barriers in different side directions are closely related to the hopping between the nearest neighbor sites. The periodic potential distribution for an anisotropic triangular lattice is shown in Fig. 1. Then fermionic atoms in the two-hyperfine manifold, such as ^{40}K, can be loaded into the lattice potential by combining different cooling methods, including laser cooling and evaporative cooling. The interactions between the fermions can be tuned by the Feshbach resonance.[9,27]

Herein we investigate the fermionic cold atoms in an anisotropic triangular optical lattice by combining the dynamical cluster approximation (DCA)[28] with the continuous time quantum Monte–Carlo method.[29] It is well known that the self energy in the general dynamical mean-field theory (DMFT) is exact in the infinite-dimensional limit and a good approximation for three dimensions.[30] However, the dynamical cluster approximation method is very efficient in the treatment of the nonlocal correlation, which plays a significant role in frustrated systems. In the dynamical cluster approximation method, the lattice problem is mapped into a self-consistently embedded finite-sized cluster and the irreducible quantities of the embedded cluster are used as an approximation for the corresponding lattice quantities. The continuous time quantum Monte–Carlo method is used as an impurity solver.

*Project supported by the National Natural Science Foundation of China (Grant Nos. 11074141, 11174169, and 10934010), the National Natural Science Foundation of China and Research Grant Council (NSFC/RGC) Joint Research Scheme (Grants No. 11061160490), and the National Basic Research Program of China (Grants Nos. 2011CB921502, 2012CB821305, 2010CB922904, 2009CB930701, and 2009CB929202).

†Corresponding author. E-mail: ba09@mails.tsinghua.edu.cn

© 2013 Chinese Physical Society and IOP Publishing Ltd

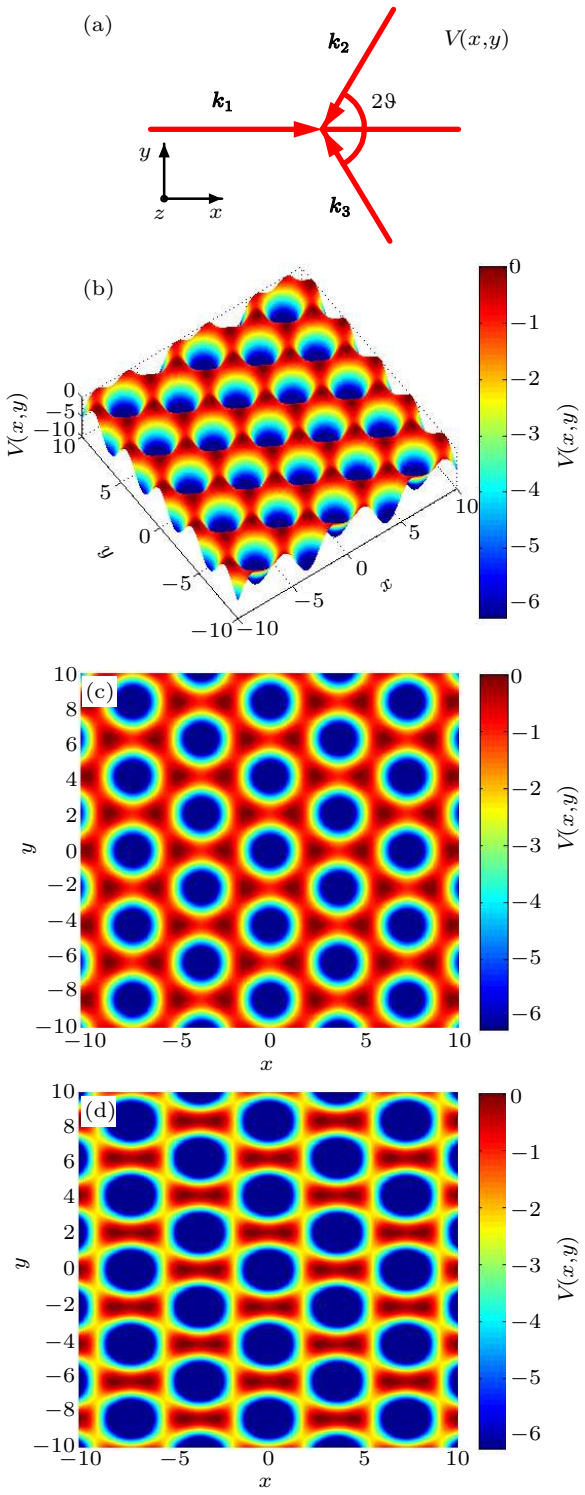


Fig. 1. (color online) (a) Sketch of the propagation directions of the laser beams used. (b) Sketch of potential $V(x,y)$ for the case of an isotropic triangular lattice. (c) Potential distribution of an isotropic triangular lattice, $t_1 = t_2 = t_3$. (d) Potential distribution of an anisotropic triangular lattice, $t_2 = t_3 = t_1/3$.

This paper is organized as follows. In Section 2, the artificial anisotropic triangular lattice with fermionic atoms and the algorithm and method used to describe such an artificial system are discussed in detail. In Section 3, we present the double occupancy and the density of states of the system. The Fermi surface evolution, the temperature–interaction (T–U) phase diagram, and the competition between the anisotropic parameters λ and the interaction are also shown. In Section 4, we design a feasible experiment for the observation of the quantum phase transitions of the cold fermionic atoms in an anisotropic triangular optical lattice in which the hopping terms are geometrically equilateral but anisotropic.

2. Anisotropic triangular optical lattice

An artificial anisotropic triangular optical lattice, which is equilateral in the geometry but anisotropic in the periodic potential in different directions, can be created by the interference of three laser beams with the same wavelength $\lambda = 1064$ nm and different amplitudes in different propagating directions. The lasers are in the xy plane, and they are all polarized in the z direction, separated by $2\pi/3$ from each other. The electric fields are $\boldsymbol{E}_1 = \boldsymbol{E}_{01}\cos(\boldsymbol{k}_1\cdot\boldsymbol{r} - \omega t + \varepsilon_1)$, $\boldsymbol{E}_2 = \boldsymbol{E}_{02}\cos(\boldsymbol{k}_2\cdot\boldsymbol{r} - \omega t + \varepsilon_2)$, and $\boldsymbol{E}_3 = \boldsymbol{E}_{03}\cos(\boldsymbol{k}_3\cdot\boldsymbol{r} - \omega t + \varepsilon_3)$, respectively. In our previous work,[24] the most special case of $\boldsymbol{E}_{01} = \boldsymbol{E}_{02} = \boldsymbol{E}_{03} = \boldsymbol{E}_0$ has been studied; here a more general case in which the amplitudes of the lasers used satisfy $\boldsymbol{E}_{01} = \boldsymbol{E}_0 > \boldsymbol{E}_{02} = \boldsymbol{E}_{03} = \boldsymbol{E}_0/n$, ($n \subseteq \mathbf{R}$) is discussed systematically. We obtain an anisotropic triangular optical lattice through adjusting the amplitudes of the lasers used. For simplicity, we set the initial phase $\varepsilon_1 = \varepsilon_2 = \varepsilon_3 = 0$. Therefore, the confining potential in the xy plane is

$$V(x,y) = V_0\Big[\frac{1}{2} + \frac{1}{n^2}\Big(1 + 2n\cos\Big(\frac{3kx}{2}\Big)\cos\Big(\frac{\sqrt{3}ky}{2}\Big) + \cos\big(\sqrt{3}ky\big)\Big)\Big], \tag{1}$$

where V_0 is a constant which relates to the maximum depth of the lattice potential in the xy plane and is given in units of recoil energy $E_r = h^2/(2m\lambda^2)$, here h is Planck's constant, m is the atomic mass, and λ is the wavelength of the laser beam. The anisotropic hopping terms along different lattice directions, i.e., t_1, t_2, and t_3 shown in Fig. 2(a), can be achieved through adjusting parameter n^2 ($n \in \mathbf{R}$) that relates to the ratio between the amplitudes of the laser beams used. Fermionic ^{40}K atoms in the two-hyperfine manifold are loaded into the triangular optical lattice in the same percentage through evaporative cooling at a magnetic bias field of 203.06 G.[5] Both the non-interacting regime with a scattering length of $a = (0 \pm 10)a_0$ and the repulsive on-site interactions between fermionic atoms can be tuned by the Feshbach resonance, where a_0 is the Bohr radius.

The physics of the fermions with on-site repulsive interaction in an anisotropic triangular optical lattice in the half filled case can be described well by the celebrated anisotropic Hubbard model, and the Hamiltonian is

$$H = -\sum_{\langle i,j\rangle\sigma} t_{ij}c^{+}_{i\sigma}c_{j\sigma} + U\sum_i n_{i\uparrow}n_{i\downarrow}, \tag{2}$$

where $c_{i\sigma}^{+}$ and $c_{i\sigma}$ represent the creation and the annihilation operators of fermions on lattice site i, respectively, and $n_{i\sigma} = c_{i\sigma}^{+}c_{i\sigma}$ is the density operator of fermions. The general formula for the hopping terms is $t_i = (4/\sqrt{\pi})E_r(\alpha_i V_0/E_r)^{3/4}\exp[-2(\alpha_i V_0/E_r)^{1/2}]$, $(\alpha_i \in \mathbf{R}, i = 1,2,3)$, α_i is a parameter that adjusts the confining potential in different direction. The different hopping terms in different directions can be achieved by adjusting α_i, and $U = \sqrt{8/\pi}ka_s E_r(V_0/E_r)^{3/4}$ is the on-site repulsive interaction, which can be tuned by the Feshbach resonance.

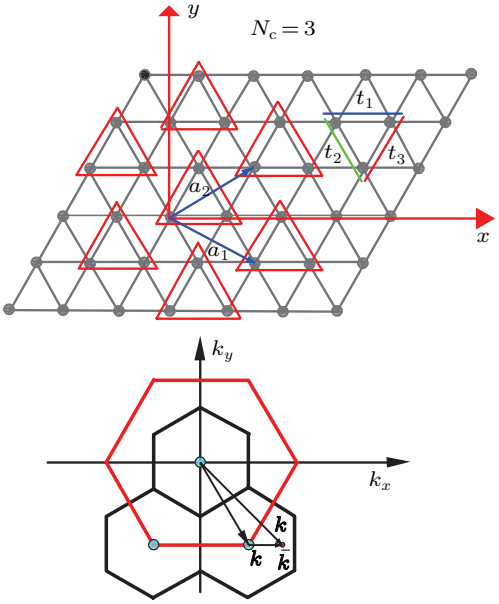


Fig. 2. (color online) (a) Sketch of an anisotropic triangular lattice, here t_1, t_2, and t_3 are the hopping strengths along different directions. (b) Coarse graining procedure in the first Brillouin zone when $N_c = 3$. The red part shows the first Brillouin zone. The three black hexagons show the region of divided Brillouin zone for DCA calculation.

In the dynamical cluster approximation, the lattice problem is mapped onto a self-consistently embedded finite-sized cluster, and the reciprocal space of the lattice containing N points is divided into finite cells. The coarse-graining Green's function $\overline{G}$ is obtained by averaging Green's function G within each cell. The coarse graining procedure of the anisotropic triangular lattice in the DCA is illustrated as follows. As shown in Fig. 2, the lattice problem of the anisotropic triangular lattice is mapped onto a three-site cluster, so the Brillouin zone is divided into 3 cells and each cell is represented by a cluster momentum $\boldsymbol{K}$. The coarse-grained Green's function is

$$\overline{G}(\boldsymbol{K}, \mathrm{i}\omega_n) = \frac{N_c}{N}\sum_{\boldsymbol{k}} \frac{1}{\mathrm{i}\omega_n - \varepsilon_{\boldsymbol{K}+\boldsymbol{k}} - \overline{\Sigma_\sigma}(\boldsymbol{K}, \mathrm{i}\omega_n)}, \tag{3}$$

where the summation over $\boldsymbol{k}$ is taken within the coarse-graining cell, and the ω_n is the Matsubara frequency.

After mapping the lattice problem onto the finite-size cluster, we use the continuous time quantum Monte–Carlo method (CTQMC) as the impurity solver to deal with the cluster problem. The CTQMC does not use the Trotter decomposition and is more exact than the determinantal QMC. We carry out 10^7 sweeps in our CTQMC step. The process from

$$\overline{G}(\boldsymbol{K}, \mathrm{i}\omega_n) = \frac{N_c}{N}\sum_{\boldsymbol{k}} 1/(\mathrm{i}\omega_n - \varepsilon_{\boldsymbol{K}+\boldsymbol{k}} - \overline{\Sigma_\sigma}(\boldsymbol{K}, \mathrm{i}\omega_n))$$

to

$$\Sigma_c(\boldsymbol{K}, \mathrm{i}\omega_n) = \overline{\mathcal{G}}(\boldsymbol{K}, \mathrm{i}\omega_n)^{-1} - \overline{G}(\boldsymbol{K}, \mathrm{i}\omega_n)^{-1}$$

is repeated until $\Sigma_c(\boldsymbol{K}, \mathrm{i}\omega_n)$ converges to the required accuracy, as shown in Fig. 3.

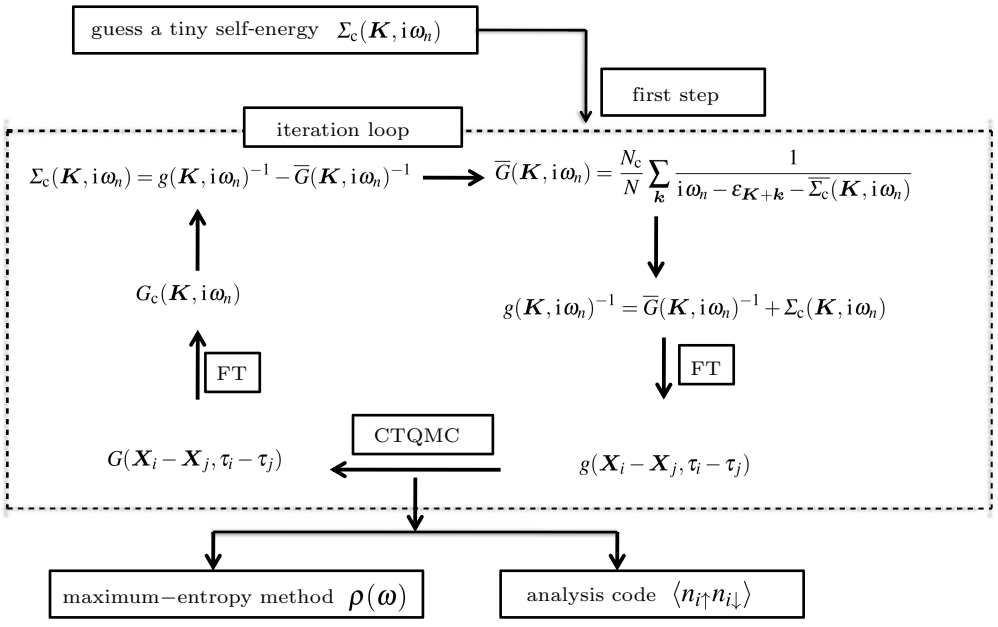


Fig. 3. Flow diagram of continuous time quantum Monte–Carlo iteration loop, here FT represents the Fourier transformation.

3. Phase diagram

We calculate the double occupancy and the density of states of the fermionic cold atoms in the anisotropic triangular optical lattice. We also show the Fermi surface's evolution of the system at a fixed temperature and the repulsive interactions and the phase diagram of the system.

The double occupancy $D_{\rm occ} = \partial F/\partial U = \frac{1}{4}\sum_i \langle n_{i\uparrow} n_{i\downarrow}\rangle$ as a function of interaction U for various temperatures and different hopping terms has been investigated, where F is the free energy. We introduce anisotropic parameter $\lambda = t_1/t_i$ (i = 2,3), which can describe the degree of anisotropy of the triangular lattice. As shown in Fig. 4(a), for a fixed temperature $T = 0.5$ ($T = 0.25$), the anisotropy of the lattice is suppressed when U/t_i is larger than 18.0 (15.0). From Fig. 4(b), we can see that the effect of temperature on $D_{\rm occ}$ weakens due to the suppression of the itinerancy of atoms with the increase of the interaction and vanishes when U/t_i is larger than 8.0 for $\lambda < 1$ and 15.0 for $\lambda > 1$.

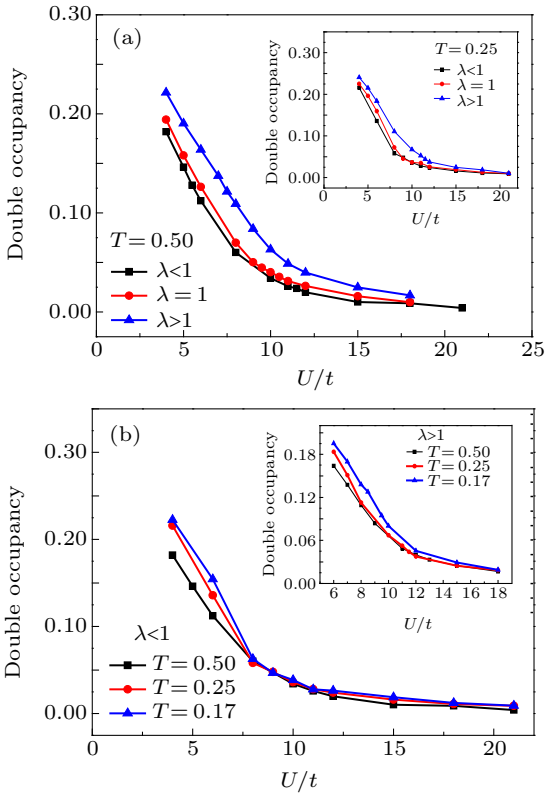


Fig. 4. (color online) The double occupancy $D_{\rm occ}$ as a function of the interaction U for different temperatures and different λ, where $\lambda = t_1/t_{2,3}$ and $t_2 = t_3$. (a) The double occupancy versus the interaction at a fixed temperature $T = 0.5$ (inset: $T = 0.25$) with different anisotropic parameter λ. (b) The double occupancy versus the interaction at different temperatures for $\lambda < 1$ (inset: $\lambda > 1$).

The density of states $\rho(\omega)$ (DOS) is calculated by using the maximum entropy method.[31] As shown in Fig. 5, at $T = 0.5$, the formation processes of the pseudogap for $t_1 = 0.8$ and $t_1 = 1.5$ are different. For $T = 0.5$ and $t_1 = 0.8$, the pseudogap directly forms by splitting the Fermi-liquid-like peak at $U/t_i = 7.0$ without the appearance of a sharp quasiparticle peak with two shoulders, named the Kondo peak, which appears for $T = 0.5$ and $t_1 = 1.5$. In the metal phase region, a concave curve which is named the pseudogap appears between two quasi-symmetric peaks around the Fermi level after the appearance of the Kondo peak at $U/t_i = 10.0$. At $T = 0.5$, the system is transferred to an insulator state when $U_c/t_i = 10.0$ for $t_1 = 0.8$ and $U_c/t_i = 12.5$ for $t_1 = 1.5$. At $T = 0.25$, the Kondo resonance peak, which is characterized by a sharp quasi-particle peak with two shoulders, appears at $U_c/t_i = 6.5$ for $t_1 = 0.8$ and $U_c/t_i = 8.5$ for $t_1 = 1.5$. A gap is opened when the interaction is stronger than the critical interaction $U_c/t_i = 9.5$ for $t_1 = 0.8$ and $U_c/t_i = 11.8$ for $t_1 = 1.5$. At low temperatures, the Kondo peak is formed due to the interaction between the local atom and the itinerant atom.

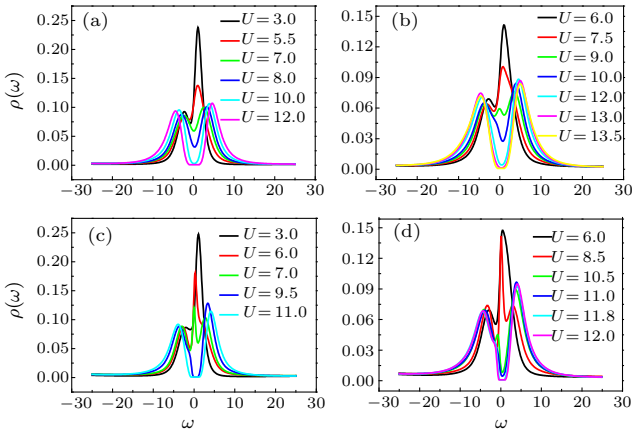


Fig. 5. (color online) The density of states as a function of frequency ω for different interaction U/t_i ($i = 2,3$), the parameters are (a) $T = 0.5, t_1 = 0.8$; (b) $T = 0.5, t_1 = 1.5$; (c) $T = 0.25, t_1 = 0.8$; and (d) $T = 0.25, t_1 = 1.5$.

The Fermi surface's evolution for different t_1 at fixed $t_2 = t_3 = 1$ is shown in Fig. 6, where $T/t_i = 0.25$ and $U/t_i = 8.0$ ($i = 2,3$). The spectral function is given by $A(k;\omega = 0) \approx -\lim_{\omega_n \to 0} {\rm Im}G(k, {\rm i}\omega_n)/\pi$. A linear extrapolation of the first two Matsubara frequencies is used to estimate the self energy to zero frequency.[32] Due to the delocalization of the particles, the amplitude of the spectral weight becomes larger and the ring breadth becomes narrow and distinct with the increase of t_1 at the fixed temperature and interaction. The Fermi surface becomes a nearly flat plane when t_1 is lower than 1.0 at $T = 0.25$. The transition from the Fermi liquid to the Mott insulator is much faster at low temperature than that at relatively high temperature.

The temperature–interaction (T–U) phase diagram and the competition between anisotropic parameter λ and the interaction of cold atoms in the anisotropic triangular optical lattice are shown in Fig. 7. With the increase of t_1, the corresponding transitions entirely shift to larger interactions and lower temperatures. For $t_1 = 0.8$, there is no Kondo peak between the Fermi liquid and the pseudogap until T is lower than 0.45. With the increase of t_1 at fixed $t_2 = t_3 = 1$, the Kondo peak not only appears but the gap between the Kondo peak

and the pseudogap becomes nearly zero. When the interaction is stronger than the critical value of interaction for the Mott transition, the system translates into the Mott insulator, which is confirmed by the opened gap. The pseudogap is suppressed at low temperatures due to the Kondo effect. The competition between anisotropic parameter λ and the interaction at $T/t_i = 0.5$ in Fig. 7(d) shows that with the increase of the interaction, the transition points λ for the Fermi liquid to the Mott insulator increase and the slope decreases.

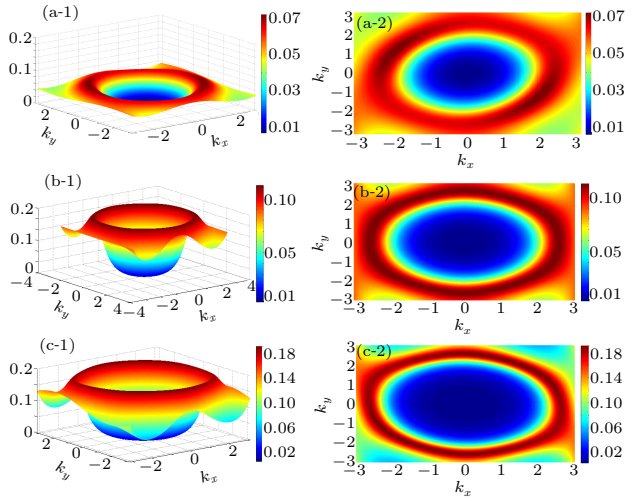


Fig. 6. (color online) The Fermi surface for (a) $t_1 = 0.5$, (b) $t_1 = 1.0$, and (c) $t_1 = 1.5$ at $t_2 = t_3 = 1$, $T = 0.25$, and $U/t_i = 8.0$ $(i = 2,3)$.

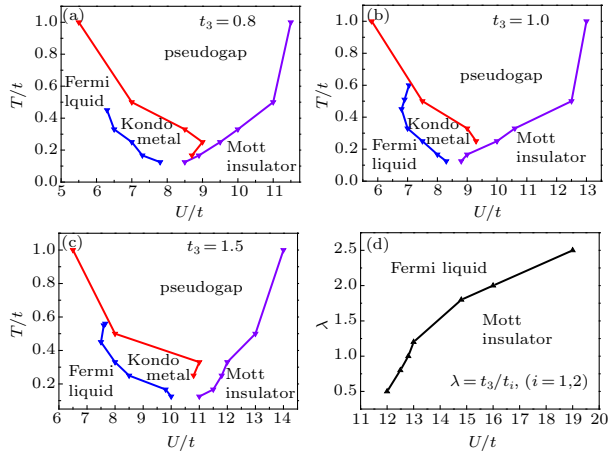


Fig. 7. (color online) The temperature–interaction phase diagrams of fermionic cold atoms in the anisotropic triangular optical lattice for (a) $t_1 = 0.8$, (b) $t_1 = 1.0$, and (c) $t_1 = 1.5$. (d) The competition between $\lambda = t_1/t_i$ $(i = 2,3)$ and interaction U.

4. Experiment proposal

We propose an experiment scheme for the observation of the quantum phase transition of fermionic cold atoms in a geometrically frustrated anisotropic triangular optical lattice. First, we use three laser beams of wavelength $\lambda = 1064$ nm in the same plane with different amplitudes to create the anisotropic triangular optical lattice. The included angle between each two laser beams equals $2\pi/3$. A balanced mixture of the fermionic ^{40}K atoms in two hyperfine manifold states, states $|m_F\rangle = |-9/2\rangle$ and $|-7/2\rangle$, is prepared through evaporative cooling at a magnetic bias field.[33] Then a spin mixture of atoms in the $|-9/2\rangle$ and $|-5/2\rangle$ states can be loaded into the optical lattice potentials through tuning the scattering length to the desired value by the Feshbach resonance.[34–37] We can achieve the zero interaction regime with a scattering length of $a = (0 \pm 10)a_0$. The repulsive on-site interaction U/t_i between the atoms can be obtained by transferring the atoms in the $|-7/2\rangle$ state to the $|-5/2\rangle$ state during the evaporation cooling.

With the increase of the interaction, the system will transform from Fermi liquid ($a_s < 48a_0$) to Mott insulator ($a_s > 111a_0$) at $T = 5.96$ nK for lattice depth $V_0 = 10E_r$, where a_s indicates the s-wave scattering length which is used to determine the effective interaction region. In order to detect the double occupancy, further tunneling should be prevented through increasing the potential depth V_0 of the optical lattice rapidly and the energies of the atoms on the doubly occupied sites need to be shifted by approaching the Feshbach resonance. One spin component of fermions on the doubly occupied sites is transferred to an unpopulated magnetic sublevel by using a radio-frequency pulse. The double occupancy can be deduced by the fraction of transformed atoms obtained through the absorption imaging.[5,38] After completely turning off the confining potential, the atoms expand anisotropically for several milliseconds due to the anisotropy of the potential depth in different directions. One can obtain the Fermi surface through the absorption imaging.[39,40]

5. Conclusion

We investigate the quantum phase transitions of fermionic cold atoms in a geometrically frustrated anisotropic triangular optical lattice by using the dynamical cluster approximation method combined with the continuous-time quantum Monte–Carlo algorithm in the frame of half-filled and one-band Hubbard model. The system transforms from Fermi liquid into Mott insulator when the repulsive on-site interaction reaches a certain value for a fixed temperature. We also observe the Kondo effect which results in the suppression of the pesudogap at low temperatures. It is found that the anisotropy of the lattice is suppressed when U/t_i reaches a critical value for a fixed temperature and with the increase of t_1 at fixed $t_2 = t_3$, the transition lines shift to larger interactions and lower temperatures.

References

[1] Petsas K I, Coates A B and Grynberg G 1994 *Phys. Rev. A* **50** 5173
[2] Greiner M and Fölling S 2008 *Nature* **453** 736
[3] Jaksch D and Zoller P 2005 *Ann. Phys.* **315** 52
[4] Bloch I, Dalibard J and Zwerger W 2008 *Rev. Mod. Phys.* **80** 885

[5] Jördans R, Strohmaier N, Günter K, Moritz H and Esslinger T 2008 *Nature* **455** 204
[6] Gemelke N, Zhang X, Hung C L and Chin C 2009 *Nature* **460** 995
[7] Helmes R W, Costi T A and Rosch A 2008 *Phys. Rev. Lett.* **100** 056403
[8] Hofstetter W, Cirac J I, Zoller P, Demler E and Lukin M D 2002 *Phys. Rev. Lett.* **89** 220407
[9] Chin C, Grimm R, Julienne P and Tiesinga E 2010 *Rev. Mod. Phys.* **82** 1225
[10] Greiner M, Mandel O, Esslinger T, Hänsch T W and Bloch I 2002 *Nature* **415** 39
[11] Simon J, Bakr W S, Ma R, Tai M E, Preiss P M and Greiner M 2011 *Nature* **472** 307
[12] Wei D, Xiong D Z and Chen H X 2007 *Chin. Phys. Lett.* **24** 1541
[13] Struck J, Ölschläger C, Le Targat R, Soltan-Panahi P, Eckardt A, Lewenstein M, Windpassinger P and Sengstock K 2011 *Science* **333** 996
[14] Shimizu Y, Miyagawa K, Kanoda K, Maesato M and Saito G 2003 *Phys. Rev. Lett.* **91** 107001
[15] Harris M J, Bramwell S T, McMorrow D F, Zeiske T and Godfrey K W 1997 *Phys. Rev. Lett.* **79** 2554
[16] Kurosaki Y, Shimizu Y, Miyagawa K, Kanoda K and Saito G 2005 *Phys. Rev. Lett.* **95** 177001
[17] Castelnovo C, Moessner R and Sondhi S L 2008 *Nature* **451** 42
[18] Ohashi T, Momoi T, Tsunetsugu H and Kawakami N 2008 *Phys. Rev. Lett.* **100** 076402
[19] Yoshioka T, Koga A and Kawakami N 2009 *Phys. Rev. Lett.* **103** 036401
[20] Duan L M, Demler E and Lukin M D 2003 *Phys. Rev. Lett.* **91** 090402
[21] Duan L M 2005 *Phys. Rev. Lett.* **95** 243202
[22] Wu W, Chen Y H, Tao H S, Tong N H and Liu W M 2010 *Phys. Rev. B* **82** 245102
[23] Chen Y H, Tao H S, Yao D X and Liu W M 2012 *Phys. Rev. Lett.* **108** 246402
[24] Chen Y H, Wu W, Tao H S and Liu W M 2010 *Phys. Rev. A* **82** 043625
[25] Santos L, Baranov M A, Cirac J I, Everts H U, Fehrmann H and Lewenstein M 2004 *Phys. Rev. Lett.* **93** 030601
[26] Schneider U, Hackermüller L, Will S, Best Th, Bloch I, Costi T A, Helmes R W, Rasch D and Rosch A 2008 *Science* **322** 1520
[27] Chai S J, Wang P J and Fu Z K 2011 *Chin. Phys. B* **20** 103401
[28] Maier T, Jarrell M, Pruschke T and Hettler M H 2005 *Rev. Mod. Phys.* **77** 1027
[29] Rubtsov A N, Savkin V V and Lichtenstein A I 2005 *Phys. Rev. B* **72** 035122
[30] Metzner W and Vollhardt D 1989 *Phys. Rev. Lett.* **62** 324
[31] Jarrell M and Gubernatis J E 1996 *Phys. Rep.* **269** 133
[32] Parcollet O, Biroli G and Kotliar G 2004 *Phys. Rev. Lett.* **92** 226402
[33] O'Hara K M, Hemmer S L, Gehm M E, Granade S R and Thomas J E 2002 *Science* **298** 2179
[34] Regal C A, Ticknor C, Bohn J L and Jin D S 2003 *Nature* **424** 47
[35] Klempt C, Henninger T, Topic O, Will J, Ertmer W, Tiemann E and Arlt J 2007 *Phys. Rev. A* **76** 020701
[36] Loftus T, Regal C A, Ticknor C, Bohn J L and Jin D S 2002 *Phys. Rev. Lett.* **88** 173201
[37] Zwierlein M W, Schirotzek A, Schunck C H and Ketterle W 2006 *Science* **311** 492
[38] Strohmaier N, Takasu Y, Günter K, Jördens R, Köhl M, Moritz H and Esslinger T 2007 *Phys. Rev. Lett.* **99** 220601
[39] Chin J K, Miller D E, Liu Y, Stan C, Setiawan W, Sanner C, Xu K and Ketterle W 2006 *Nature* **443** 961
[40] Köhl M, Moritz H, Stöferle T, Günter K and Esslinger T 2005 *Phys. Rev. Lett.* **94** 080403